

Pre-treatment with galectin-1 attenuates lipopolysaccharide-induced myocarditis by regulating the Nrf2 pathway

Liying Shen, Kongjie Lu, Zhenfeng Chen, Yingwei Zhu, Cong Zhang, Li Zhang

Department of Cardiology, Huzhou Central Hospital, Huzhou, Zhejiang, China

ABSTRACT

Galectin-1 (Gal-1), a member of a highly conserved family of animal lectins, plays a crucial role in controlling inflammation and neovascularization. However, the potential role of Gal-1 in preventing myocarditis remains uncertain. We aimed to explore the functions and mechanisms of Gal-1 in preventing myocarditis. *In vivo*, C57/BL6 mice were pre-treated with or without Gal-1 and then exposed to lipopolysaccharide (LPS) to induce myocarditis. Subsequently, cardiac function, histopathology, inflammation, oxidative stress, and apoptosis of myocardial tissues were detected. Following this, qRT-PCR and Western blotting were applied to measure iNOS, COX2, TXNIP, NLRP3 and Caspase-1 p10 expressions. *In vitro*, H9c2 cells pre-treated with different doses of Gal-1 were stimulated by LPS to induce myocarditis models. CCK8, flow cytometry and reactive oxygen species (ROS) assay were then employed to estimate cell viability, apoptosis and oxidative stress. Furthermore, Nrf2 and HO-1 protein expressions were evaluated by Western blotting *in vivo* and *in vitro*. The results showed that *in vivo*, Gal-1 pre-treatment not only moderately improved cardiac function and cardiomyocyte apoptosis, but also ameliorated myocardial inflammation and oxidative damage in mice with myocarditis. Furthermore, Gal-1 inhibited TXNIP-NLRP3 inflammasome activation. *In vitro*, Gal-1 pre-treatment prevented LPS-induced apoptosis, cell viability decrease and ROS generation. Notably, Gal-1 elevated HO-1, total Nrf2 and nuclear Nrf2 protein expressions both *in vivo* and *in vitro*. In conclusion, pre-treatment with Gal-1 exhibited cardioprotective effects in myocarditis *via* anti-inflammatory and antioxidant functions, and the mechanism may relate to the Nrf2 pathway, which offered new solid evidence for the use of Gal-1 in preventing myocarditis.

Key words: Galectin-1; lipopolysaccharide; myocarditis; Nrf2; TXNIP-NLRP3 inflammasome.

Correspondence: Li Zhang, Department of Cardiology, Huzhou Central Hospital, No.1558, Sanhuan North Road, Wuxing District, 313000 Huzhou, Zhejiang, China. E-mail: zhanglinbu2010@163.com

Contributions: LZ, KL, ZC, designed the research; LS, YZ, CZ, acquired and analyzed data; ZC, obtained the funding; LS, drafted the manuscript; LS, LZ, revised the manuscript for important intellectual content. All authors contributed significantly, read and approved the final version of the manuscript and agreed to be accountable for all aspects of the work.

Conflict of interest: the authors declare no conflict of interest.

Ethical approval: all animal experiments were performed according to the guidelines of laboratory animal care and were approved by the Animal Experimentation Ethics Committee of Zhejiang Eyong Pharmaceutical Research and Development Center, Hangzhou, China (approval no. ZJEY-20220217-04).

Availability of data and material: the datasets used during the present study are available from the corresponding author on reasonable request.

Funding: this work was supported by the Huzhou Cardiovascular and Cerebrovascular Disease Discipline Group (grant number XKQ-HT-202102A) and Huzhou City Public Welfare Application Research Project (grant number 2023GY10). The funding source played no role in study design, collection, analysis and interpretation of data, writing of the report and decision to submit the article for publication.

Introduction

Myocarditis, a common disorder characterized by the presence of inflammation in the myocardium, is the leading cause of sudden death in young patients.¹ Myocarditis treatment remains difficult and challenging due to the proliferation of inflammatory lesions in the myocardium.² Heart transplantation, implantable cardioverter defibrillators, intravenous immunoglobulin, drug therapy, and biotherapy are currently available treatments for myocardial dysfunction.³ However, patients who recover initially after receiving these treatments may experience a relapse of myocardial dysfunction years later, endangering their health. If the relapse is severe, patients will develop heart failure or even death.⁴ Hence, more in-depth research is required to investigate novel and safe drugs for preventing myocarditis.

Galectins are a groups of protein that can specifically bind to β -galactosides.⁵ To date, a total of 15 mammalian galectins have been discovered in different organs and tissues.⁶ Galectin-1 (Gal-1) is an isoform of galectin, has been reported to be associated with many cell functions, such as proliferation, apoptosis, adhesion and migration.⁷ The main physiological function of Gal-1 is to serve as an anti-inflammatory mediator to inhibit immune responses.⁸ Previous studies have demonstrated the efficacy of Gal-1 in reducing inflammation in cardiovascular pathophysiology.⁹ It has been reported that Gal-1-deficient mice exhibit enhanced cardiac inflammation after acute myocardial infarction.¹⁰ However, evidence for the roles and mechanisms of Gal-1 in preventing lipopolysaccharide (LPS)-induced myocarditis is limited.

Hence, in the research, both *in vivo* and *in vitro* experiments were conducted to explore the functions and mechanisms of Gal-1 in LPS-induced myocarditis. Our findings demonstrated that Gal-1 had the potential to prevent LPS-caused myocarditis inflammation and oxidative stress, potentially by regulating the nuclear factor erythroid 2-related factor 2 (Nrf2) pathway and suppressing thioredoxin interacting protein (TXNIP)-nucleotide-binding oligomerization domain (NOD)-like receptor protein 3 (NLRP3) inflammasome activation. All of these indicated that pre-treatment with Gal-1 may be an underlying strategy for preventing acute myocarditis.

Materials and Methods

Animals

C57/BL6 male mice (aged 8 weeks), were obtained from Shanghai Lingchang Biotech Co., Ltd. (China). The mice were housed under controlled conditions with a temperature of $23\pm 2^{\circ}\text{C}$, humidity between 55-70%, and a 12 h light/dark cycle. All mice received water and food *ad libitum*. All animal experiments were performed according to the guidelines of laboratory animal care and were approved by the Animal Experimentation Ethics Committee of Zhejiang Eyong Pharmaceutical Research and Development Center (approval no. ZJEY-20220217-04, Hangzhou, China).

In vivo study

Pre-treatment with Gal-1 and establishment of myocarditis model

The C57BL/6 mice were assigned into the following groups randomly: the control group, model group, Gal-1 (50 $\mu\text{g}/\text{kg}$) group, Gal-1 (100 $\mu\text{g}/\text{kg}$) group and Gal-1 (200 $\mu\text{g}/\text{kg}$) group. There were

6 mice in each group. Mice of the Gal-1 groups or model group were intraperitoneally injected with different dosages of Gal-1 or 0.9% saline 1 h before LPS intervention (10 mg/kg, *i.p.*), as reported in published studies.¹¹ After treatment with LPS for 12 h, the mice were anesthetized using 3% isoflurane, and ultrasound M-mode echocardiography (IE33, Philips, Amsterdam, The Netherlands) was carried out as soon as possible to evaluate the cardiac function of the mice. After that, the mice were euthanized by CO_2 -inhalation, and blood was drawn from the abdominal vein and centrifuged to obtain serum for subsequent experiments. Additionally, the myocardial tissues of the mice were also processed for the following research.

Echocardiographic assessment

Echocardiographic assessments were carried out to examine the roles of Gal-1 on the cardiac function of mice with myocarditis. In brief, the mice were fixed on the operating table and their hair was shaved. Then, the mice were anesthetized by isoflurane and placed on a heating pad to maintain a heart rate of 400-500 beats/min. Following this, the pre-warmed ultrasound gel was rubbed on the chest of mice, and an ultrasound probe was applied for echocardiography measurements. Left ventricular end-systolic diameter (LVESD) and left ventricular end-diastolic diameter (LVEDD) were measured via two-dimensional M-mode ultrasonography. Left ventricular ejection fraction (LVEF), and left ventricular short-axis shortening (LVFS) were calculated using a computer algorithm, and all examinations were based on 6 consecutive cardiac cycles.

Myocardial morphometry analysis

Pathological injury of myocardial tissues was tested by hematoxylin and eosin (H&E) staining. The harvested myocardial tissues were fixed with 4% paraformaldehyde, embedded in paraffin, and then sectioned into slices with a thickness of 5 μm . Thereafter, the samples were processed with H&E staining (H3136, E4009, sigma, USA) and observed with a light microscope (Eclipse Ci-L, Nikon, Tokyo, Japan) using 40 \times and 80 \times objective. Myocardial injury was scored according to the following pathology scoring criteria: 0 point = no damage was observed in the myocardial tissues; 1 point = slight damage was observed in the myocardial tissues; 2 points = slight damage was observed in the myocardial tissues, furthermore, the intercellular space was enlarged slightly; 3 points = moderate injury was observed in the myocardial tissues, along with moderate enlargement of the intercellular space; 4 points = severe injury was observed in the myocardial tissues, and there was a severe enlargement of the intercellular space.

Immunohistochemistry analysis

Immunohistochemistry (IHC) analysis was conducted to evaluate the oxidative stress-regulated damage in the myocardium. Antigen retrieval was performed in 10 mM citric acid buffer at 95°C for 10 min. After that, sections were incubated in 3% H_2O_2 at 4°C for 10 min to eliminate endogenous peroxidase activity. The sections were then incubated with primary antibodies against 8-OHdG (10 $\mu\text{g}/\text{mL}$, ab48508, Abcam, Cambridge, UK) overnight at 4°C . After cleaning, the tissues were probed with secondary antibodies (ab97080, Abcam, 1:5000) at 37°C for another 30 min. Afterward, the sections were stained with a DAB to develop the color and were viewed under a light microscope (Eclipse Ci-L, Nikon, Japan) with 40 \times and 80 \times objective. Sections without the primary antibody were used as negative controls, and all immunohistochemistry experiments were performed with their respective negative controls. The positive expression rate of 8-hydroxy-2-deoxyguanosine (8-OHdG)=8-OHdG positive cell number/total cell number \times 100.

TUNEL

TUNEL assays were implemented to analyze the apoptosis of myocardial tissues. Briefly, the myocardial samples were deparaffinized with xylene, hydrated in ethanol, and repaired with protease K. Next, the slices were protected from light and treated with TUNEL kits (C1090, Beyotime Institute of Biotechnology, Shanghai, China) at 37°C. Following that, the slices were washed and incubated with converter-POD at 37°C. Afterward, 4',6-diamidino-2-phenylindole (DAPI) was utilized to counterstain the nuclei. The results of TUNEL were observed under fluorescence microscopy (DM3000, Leica, Wetzlar, Germany). The TUNEL positive cell rate = number of apoptotic cells/total cells × 100.

Measurement of serum inflammatory cytokines, malondialdehyde and superoxide dismutase

Malondialdehyde (MDA) and superoxide dismutase (SOD) are closely linked to the levels of oxidative stress, and were detected in the serum of mice by enzyme-linked immunosorbent assay (ELISA, A001-3-2, A003-1-1, Nanjing Construction Technology Co. Ltd., Nanjing, China). At the same time, inflammatory cytokines such as interleukin-1 β (IL-1 β), tumor necrosis factor- α (TNF- α) and interleukin-6 (IL-6) in serum were evaluated using ELISA kits (MM-0132M2, MM-0163M2, MM-0040M2, Enzyme Immunity Industry Ltd., China). All operating steps were performed strictly according to the instructions of the kits.

qRT-PCR

The total RNA of myocardial tissues was isolated by Trizol reagents based on kit instructions. Then, the total RNA was reversely transcribed to cDNA, amplified and analyzed by SYBR Green PCR kits (H0108041, YEASEN, China) on a CFX96 real-time system with specific primers. All the primer sequences utilized in this study were displayed in Table 1.

In vitro study

Cell culture

H9c2 cells, supplied by iCell Biotechnology Co. Ltd. (iCell-r012; Shanghai, China), were cultured in Dulbecco's modified Eagle's medium (DMEM) containing 10% fetal bovine serum (FBS) in a humidified incubator at 37°C with 5% CO₂. Then, H9c2 cells were pre-treated with different concentrations of Gal-1 for 1 h. After that, Gal-1 was washed out and LPS (10 μ g/mL) was added to the cells to evaluate the protective roles of Gal-1 *in vitro*.

Cell viability assay

The viability of H9c2 cells was assessed using cell counting kit-8 (CCK-8) kits (C0039, Beyotime). Simply put, the cells were plated on 96-well plates and cultured for 24 h. To investigate the preventative effects of Gal-1 on LPS-induced cytotoxicity, H9c2 cells were pre-treated with varying concentrations of Gal-1 (5-160 μ M) for 1 h, then, the cells were cultured with 10 μ g/mL of LPS. After being cultured for 12 h or 24 h, 10 μ L of CCK-8 solution was

added to each well. After cultivation at the cell incubator for another 1.5 h, the absorbance of the cells was detected at 450 nm using a microplate spectrophotometer.

Flow cytometric analysis of apoptotic cells

Annexin V/propidium iodide (PI) staining was employed to identify the antiapoptotic ability of Gal-1 *in vitro*. Firstly, H9c2 cells were incubated with Gal-1 (10, 20 and 40 μ M) for 1 h before LPS stimulation (10 μ g/mL). After being stimulated by LPS for 24 h, cells were cleaned and suspended with a binding buffer, followed by staining with Annexin V-FITC/PI solution (5 μ L Annexin V and 5 μ L PI) in the dark at 37°C for 15 min. After that, apoptotic cells were quantified using flow cytometry (FC500, Beckman Coulter, Inc., USA). Three compound holes were set up for each group, and each hole was assayed once.

Intracellular reactive oxygen species (ROS) assay

Intracellular ROS levels were measured according to the oxidation of 2',7'-dichlorodihydrofluorescein diacetate (DCFH-DA). Briefly, H9c2 cells were seeded into 24-well plates. After being pre-treated with Gal-1 (10, 20 and 40 μ M) for 1 h, H9c2 cells were stimulated by LPS (10 μ g/mL) for 24 h. Next, H9c2 cells were incubated with DCFH-DA solution (S0033M, Beyotime) replaced DMEM. After culture for another 20 min, extracellular DCFH-DA was discarded and washed with serum-free DMEM. Finally, cells were observed with an inverted fluorescence microscope (Ts2-FL, Nikon; 40 \times objective) using a FITC filter, and analyzed by Image J Analysis Software. Three compound holes were set up for each group, and each hole was assayed once.

Western blotting analysis

The nuclear and cytoplasmic protein extraction kits (P0028, Beyotime) were used for nuclear (for nuclear Nrf2) and cytoplasmic proteins (for cytoplasmic Nrf2) extraction. Furthermore, after treatment, the total proteins of H9c2 cells and heart tissues were isolated using radioimmunoprecipitation assay buffer (P0013B, Beyotime), loaded and run on a 10% sodium dodecyl sulfate-polyacrylamide gel electrophoresis, and transferred to polyvinylidene difluoride membranes (IPVH00010, Millipore, USA). After blocking with 5% non-fat milk, the membranes were probed with the primary antibodies overnight at 4°C. On the second day, the membranes were reacted with the secondary antibodies. Thereafter, the protein blots were developed by the enhanced chemiluminescence. Band intensities were quantified by the Image J software and normalized to β -actin. The antibodies used in the study were supplied by Abcam (USA) and all relevant information was presented in Table 2.

Statistical analysis

The study was analyzed using SPSS 20.0, and the values were displayed as means \pm SD. Three sections were analyzed for each group in H&E staining, IHC analysis as well as TUNEL assay. To ensure objectivity, all measurements were performed and analyzed blindly by two researchers per experiment. Student's *t*-test was

Table 1. Primer sequence of the genes for qRT-PCR analysis.

Gene	Forward Primer (5'-3')	Reverse Primer (5'-3')
<i>iNOS</i>	TTTGTGCGAAGTGTCAGTG	AGAAACTTCGGAAGGGAGCA
<i>COX2</i>	ATCATAAGCGAGGACCTGGG	ACCTCTCCACCAATGACCTG
<i>XNIP</i>	TCCTCAAGATGGGTGGCAAT	CCGAGAAAGTGGTCAGGTCT
<i>NLRP3</i>	CTCGCATTGGTTCTGAGCTC	AGTAAGGCCGGAATTCACCA
<i>Caspase-1</i>	TCATTTCGCGGTTGAATCC	CCAACAGGGCGTGAATACAG
β -actin	TCTTTGCAGCTCCTTCGTTG	TCCTTCTGACCCATTCCAC

employed for comparisons between groups, while one-way analysis of variance (one-way ANOVA) and Tukey tests were applied for multiple group comparisons. The Kruskal-Wallis H test was applied when variances were not homogeneous. In all cases, $p < 0.05$ was considered statistically significant.

Results

In vivo study

Pre-treatment with Gal-1 prevented cardiac function impairment in myocarditis mice

After inducing myocarditis in mice by LPS, LVESD values were raised ($p < 0.01$), whereas no obvious change was observed in LVEDD values (Figure 1 A,B). In addition, the LPS group exhib-

ited lower LVEF and LVFS percentages in comparison to the control mice (Figure 1 C,D; $p < 0.01$). Meanwhile, Gal-1 showed significant preventive effects against LPS-induced myocarditis by reducing the values of LVESD and LVEDD, and increasing the percentages of LVEF and LVFS ($p < 0.05$), especially at the concentration of 200 mg/kg.

Pre-treatment with Gal-1 prevented acute myocardial damage and inflammation in myocarditis mice

The functions of Gal-1 in the prevention of myocardial damage were evaluated by HE staining. As shown in Figure 2A, after stimulation with LPS, the myocardial tissues of the mice were damaged severely, as evidenced by severe infiltration of inflammatory cells, disorderly arrangement of cardiomyocytes and enlarged intercellular space. However, it could be seen clearly that all doses of Gal-1 could prevent LPS-caused damage to the myocardium, especially for 200 mg/kg of Gal-1. Consistently, the results of Figure 2B

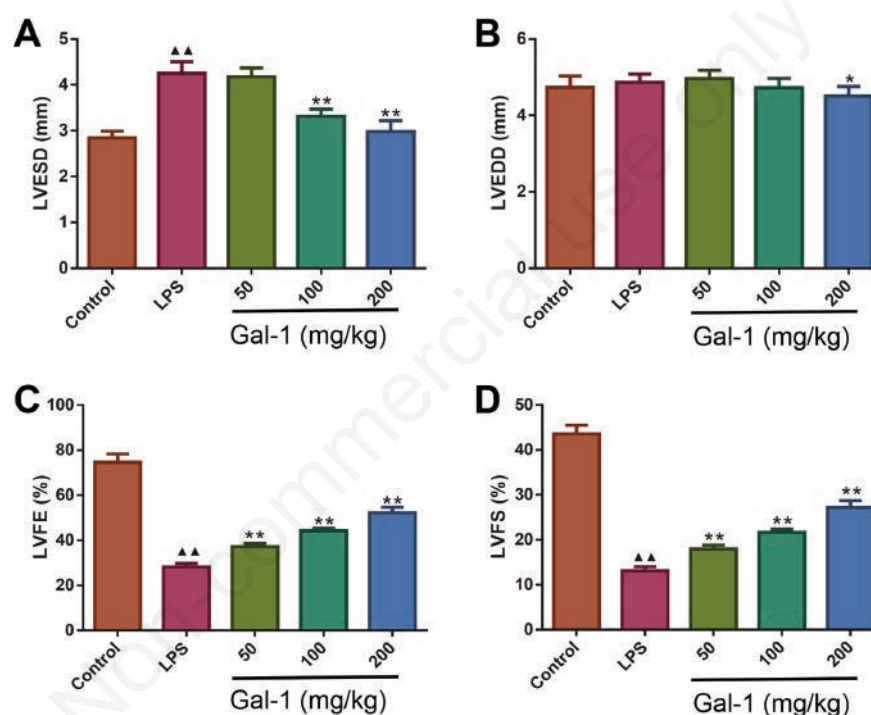


Figure 1. Pre-treatment with Gal-1 prevented cardiac function impairment and cardiac dilation in mice with LPS-induced myocarditis. **A)** LVIDd, **B)** LVIDs, **C)** EF, **D)** FS. ($\bar{x} \pm S$, $n = 6$). \blacktriangle $p < 0.05$, $\blacktriangle\blacktriangle$ $p < 0.01$ vs. Control group, * $p < 0.05$, ** $p < 0.01$ vs LPS group. Gal-1, Galectin-1; LVESD, left ventricular end-systolic diameter; LVEDD, left ventricular end-diastolic diameter; LVEF, left ventricular ejection fraction; LVFS, left ventricular short-axis shortening; LPS, lipopolysaccharide.

Table 2. Antibody information.

Antibody	Source	Cat No.	Dilutions
NLRP3	Abcam	ab214185	1:1000
Nrf2	Abcam	ab92946	1:1000
HO-1	Abcam	ab137749	1:1000
TXNIP	Abcam	ab188865	1:1000
Caspase-1+p10+p12	Abcam	ab181602	1:1000
iNOS	Abcam	ab178945	1:1000
COX2	Abcam	ab179800	1:1000
β -actin	Abcam	ab8227	1:5000

revealed that relative to the control group, the HE score of the LPS group was increased significantly, but pre-treatment with Gal-1 effectively revised the situation, especially for 200 mg/kg of Gal-1 ($p < 0.01$). To further detect the anti-inflammatory effects of Gal-1 in myocarditis, ELISA was employed to measure the levels of pro-inflammatory factors (such as IL-1 β , TNF- α and IL-6) in serum. We observed that after being stimulated with LPS, there was a significant upregulation for IL-1 β , TNF- α and IL-6 levels in serum ($p < 0.01$, Figure 2 C,E). However, Gal-1 (100 mg/kg and 200 mg/kg) pretreatment effectively inhibited the release of IL-1 β , TNF- α and IL-6 in myocarditis mice ($p < 0.05$).

Pre-treatment with Gal-1 prevented oxidative stress in myocarditis mice

As shown in Figure 3 A,B, the results of the IHC assay exhibited that LPS caused obvious 8-OHdG-labelled positive staining in the myocardium of the mice ($p < 0.01$). However, pre-treating the mice with 100 and 200 mg/kg of Gal-1 significantly reversed the situation ($p < 0.01$). At the same time, serum MDA concentration and SOD activity were also detected by ELISA kits (Figure 3 C,D). Compared to the LPS mice, the mice that received pre-treatment of 100 and 200 mg/kg of Gal-1 exhibited reduced MDA concentrations and increased SOD activity ($p < 0.05$).

Pre-treatment with Gal-1 prevented myocardial apoptosis in myocarditis mice

The anti-apoptotic effects of Gal-1 on LPS-stimulated myocarditis were assessed through TUNEL staining. As displayed in Figure 4, there were very few apoptotic cells in the myocardium of control mice, whereas apoptotic cells were massively increased following model establishment ($p < 0.01$). However, pre-treatment with 100 and 200 mg/kg Gal-1 could effectively prevent myocar-

dial apoptosis in LPS-stimulated mice, the number of apoptotic cells was decreased obviously ($p < 0.05$).

Pre-treatment with Gal-1 inhibited NLRP3 inflammasome activation in myocarditis mice

TXNIP is a multifunctional adaptor protein for different signaling pathways, which links ROS and NLRP3 inflammasome activation.¹² To further investigate the effects of Gal-1 on the TXNIP-NLRP3 inflammasome activation, qRT-PCR as well as Western blotting were conducted. As revealed in Figure 5, inducible nitric oxide synthase (iNOS), cyclooxygenase-2 (COX2), TXNIP, NLRP3, and Caspase-1 p 10 expressions, in both mRNA and protein levels, were increased evidently in the LPS group, whereas pre-treatment with 100 and 200 mg/kg Gal-1 effectively reversed these trends ($p < 0.05$).

In vitro study

Pre-treatment with Gal-1 prevented the reduction of cell viability in LPS-stimulated H9c2 cells

CCK8 was employed to evaluate the functions of Gal-1 on the viability of LPS-stimulated H9c2 cells. The results revealed that after exposure to LPS alone for 12 and 24 h, the viability of H9c2 cells dramatically decreased ($p < 0.01$, Figure 6). However, Gal-1 pre-treatment (5-160 μ M) prevented the reduction of cell viability in a dose-dependent manner, no matter the cells were stimulated with LPS for 12 h or 24 h. Of note, the protective effect of Gal-1 on cell viability was not cumulative, no sustained upregulation was observed in cell viability when the concentration of Gal-1 was exceeded than 40 μ M. Moreover, the protective effect of Gal-1 on viability was more remarkable at 24 h than at 12 h. Therefore, 10, 20 and 40 μ M of Gal-1 as well as 24 h LPS treatment time were selected for subsequent experiments.

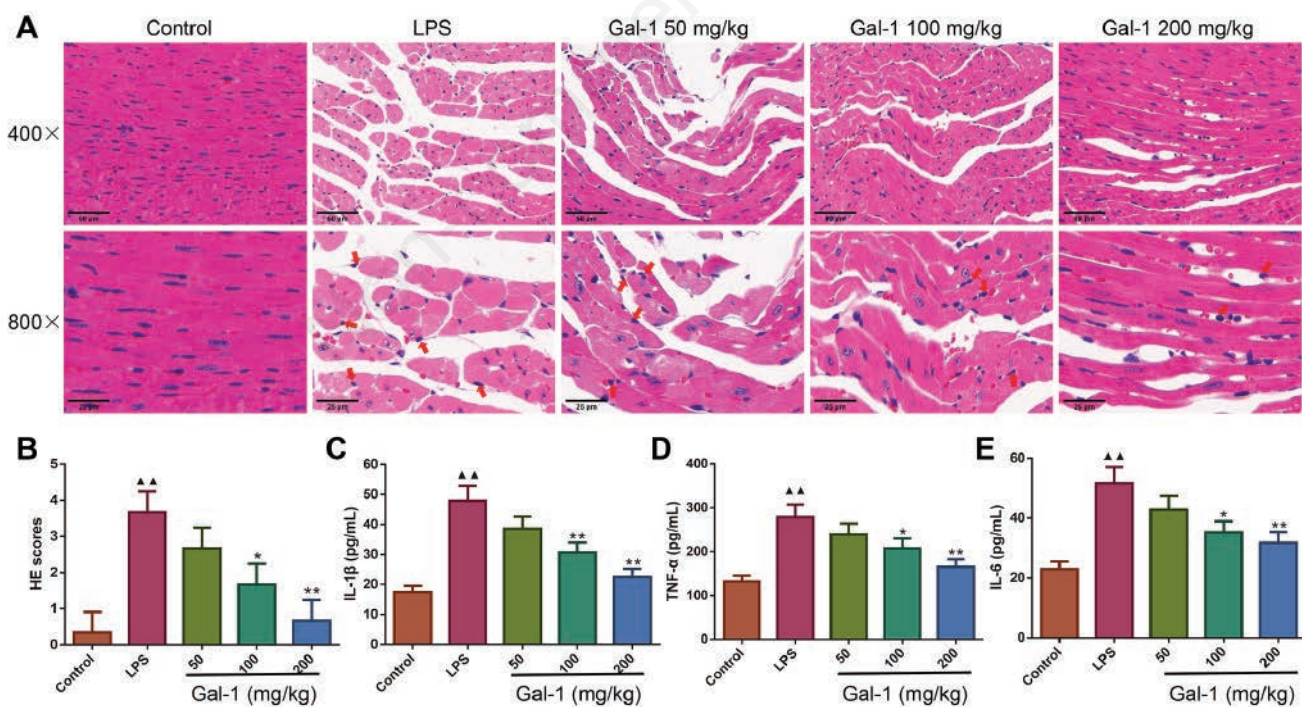


Figure 2. Pre-treatment with Gal-1 prevented histological abnormalities and inflammatory responses in myocardial tissues. **A)** Representative H&E stained images in each group (magnification: 400 \times , scale bar: 50 μ m; magnification: 800 \times , scale bar: 25 μ m). **B)** Pathological scores of myocardial tissues. **C-E)** ELISA analysis of the levels of IL-1 β , TNF- α and IL-6 in serum. ($\bar{x} \pm S$, n=3). \blacktriangle $p < 0.05$, $\blacktriangle\blacktriangle$ $p < 0.01$ vs Control group, * $p < 0.05$, ** $p < 0.01$ vs LPS group. Red arrows indicated infiltration of inflammatory cells. HE, hematoxylin and eosin; ELISA, enzyme-linked immunosorbent assay.

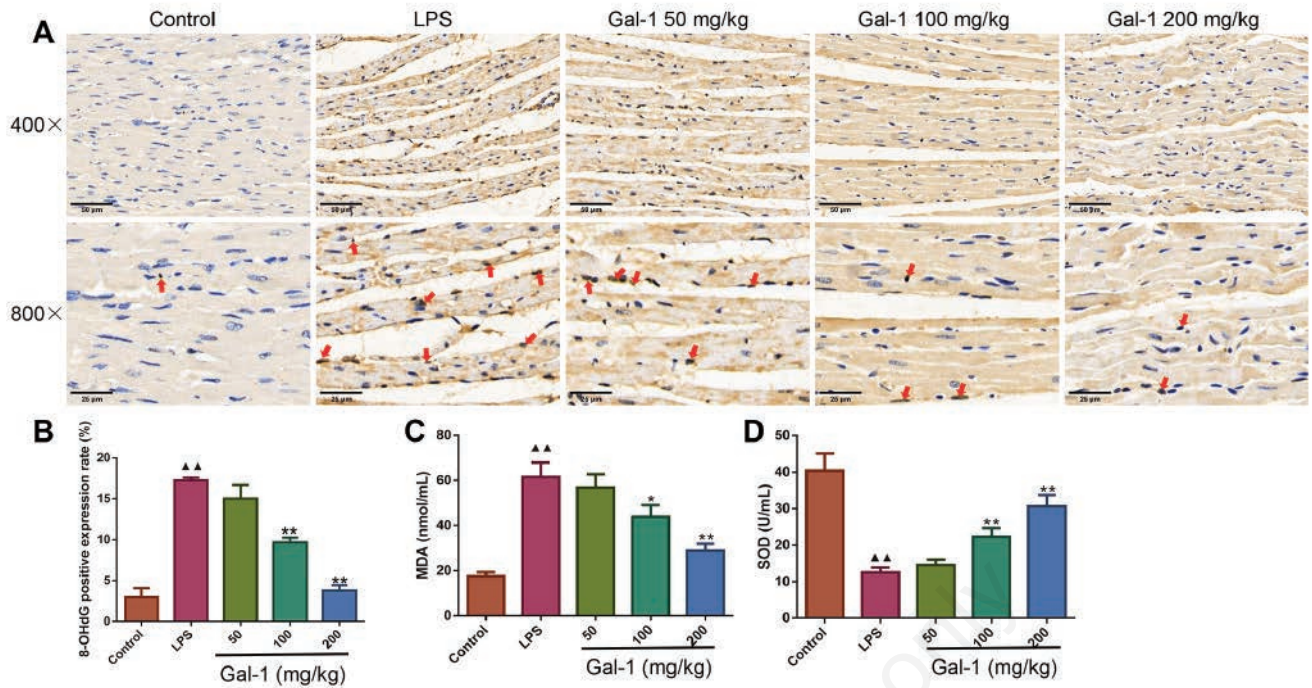


Figure 3. Pre-treatment with Gal-1 prevented oxidative stress-mediated injuries in myocardial tissues. **A)** Immunohistochemical evaluation of 8-OHdG-positive cells in myocardial tissues. (magnification: 400 \times , scale bar: 50 μ m; magnification: 800 \times , scale bar: 25 μ m). **B)** Quantitative analysis of the 8-OHdG positive index in each group. **C)** The concentration of MDA in serum. **D)** The activity of SOD in serum. ($\bar{x}\pm S$, n=3). \blacktriangle p<0.05, $\blacktriangle\blacktriangle$ p<0.01 vs Control group, *p<0.05, **p<0.01 vs LPS group. Red arrows indicated cells that were positive for 8-OHdG expression. MDA, malondialdehyde; SOD, superoxide dismutase.

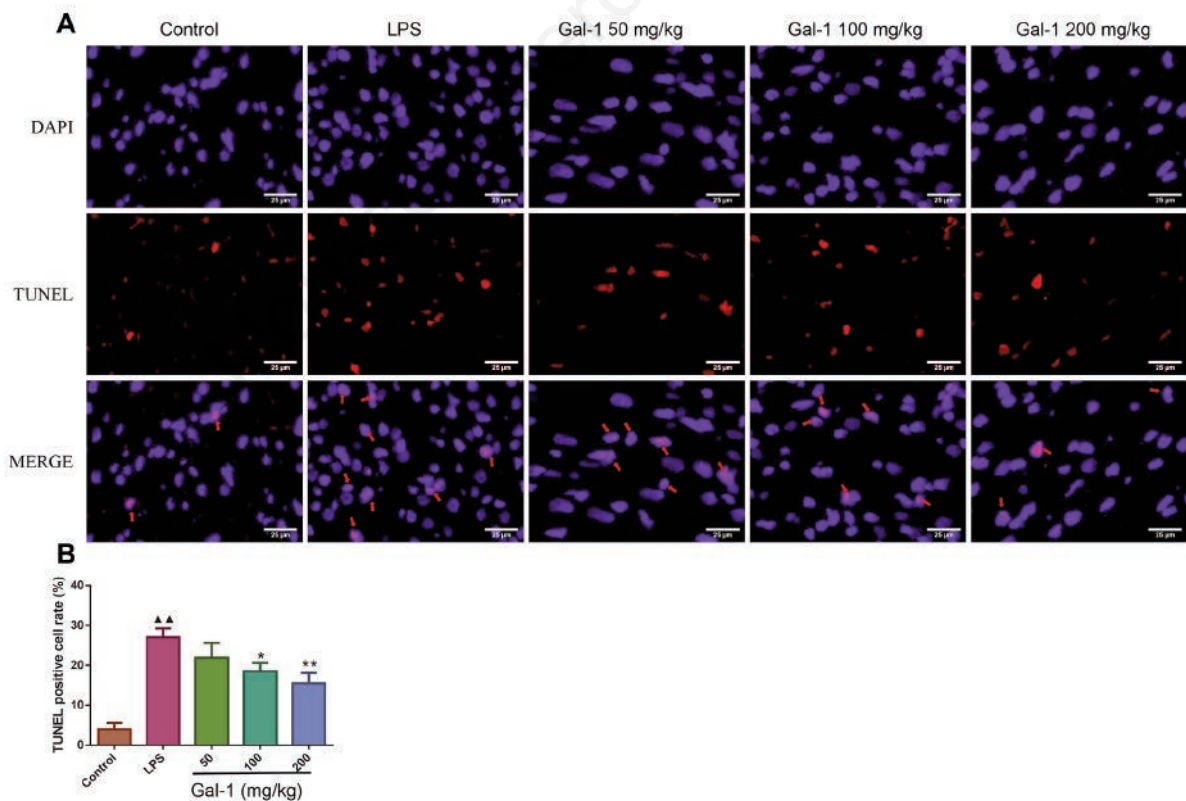


Figure 4. Pre-treatment with Gal-1 prevented myocardial apoptosis in mice with LPS-induced myocarditis. **A)** Representative images of TUNEL staining in myocardial tissues (magnification: 400 \times , scale bar: 25 μ m). **B)** Quantification of the percentage of TUNEL-positive cells. ($\bar{x}\pm S$, n=3). \blacktriangle p<0.05, $\blacktriangle\blacktriangle$ p<0.01 vs Control group, *p<0.05, **p<0.01 vs LPS group. Red arrows indicated TUNEL positive cells.

Pre-treatment with Gal-1 prevented cell apoptosis in LPS-induced H9c2 cells

Flow cytometry analysis was conducted to measure the anti-apoptotic functions of Gal-1 on LPS-induced H9c2 cells. It could be seen from Figure 7 that LPS stimulation significantly increased the apoptosis of H9c2 cells, whereas the apoptosis rate was effectively decreased in the Gal-1 groups ($p < 0.05$).

Pre-treatment with Gal-1 prevented oxidative stress in LPS-induced H9c2 cells

Due to the critical role of oxidative damage in LPS-stimulated myocardial injury, the antioxidant effect of Gal-1 was examined by DCFH-DA. As depicted in Figure 8, the fluorescence intensity of ROS was markedly increased after LPS stimulation ($p < 0.01$). It was suggested that LPS induced the generation of ROS in H9c2 cells, while the situation was rescued by pre-treating 20 μ M and 40 μ M Gal-1 ($p < 0.05$).

Pre-treatment with Gal-1 prevented LPS-caused myocardial damage via the Nrf2 pathway *in vivo* and *in vitro*

Given the Nrf2 pathway is crucial in regulating numerous antioxidant enzyme expressions, the effects of Gal-1 on the Nrf2 pathway were assessed. As presented in Figure 9, LPS treatment led to a significant reduction in total and nuclear Nrf2 protein expressions in myocardial tissues and H9c2 cells ($p < 0.01$). However, relative to the LPS group, Gal-1 pre-treatment elevated both total and nuclear Nrf2 protein expressions, while decreasing cytoplasmic Nrf2 protein expression ($p < 0.05$). It is possible that Gal-1 pre-treatment facilitated the translocation of Nrf2 from the cytoplasm to the nucleus. In addition, Gal-1 also raised the protein expression of heme oxygenase 1 (HO-1) in LPS-stimulated myocardial tissues and H9c2 cells ($p < 0.05$).

Discussion

Myocarditis, a serious ailment, could directly affect the systolic and diastolic functions of cardiomyocytes and further facilitate heart activity changes and conduction disorder.¹³ Overwhelmed inflammatory responses and excessive oxidative stress play essential roles in the pathogenesis of myocarditis.¹⁴ As is well known, myocarditis is closely associated with proinflammatory factor release and inflammatory cell infiltration.¹⁵ Furthermore, nicotinamide adenine dinucleotide phosphate (NADPH) oxidase generates a large number of free radicals to satisfy the increased oxygen consumption during myocarditis phagocytosis.¹⁶ Oxidative stress leads to cell injury and is vital in exacerbating myocardial damage.¹⁷ Additionally, oxidative stress will exacerbate inflammation and is strongly linked with myocarditis onset and progression.¹⁸ Hence, anti-inflammatory and antioxidant treatment may be beneficial for myocarditis patients.¹⁹

In the present experiment, we provided convincing evidence to demonstrate that Gal-1 prevents LPS-induced myocarditis by inhibiting inflammatory responses. *In vivo* experiments, there was remarkable inflammation in the myocardial tissues after LPS exposure. The LPS mice pre-treated with Gal-1 had less degree of histological injury, improved cardiac function as well as relieved cardiac dilation. Furthermore, Gal-1 also prevented the release of proinflammatory cytokines and the activation of TXNIP-NLRP3 inflammasome in LPS-stimulated myocarditis mice.

On the other hand, to investigate the cardioprotective roles of Gal-1 on oxidative stress, some oxidative stress biochemicals were tested. 8-OHdG, one of the modified DNA nucleoside products generated by ROS, is strongly associated with oxidative injury.²⁰ In this research, the number of 8-OHdG-positive cells was raised

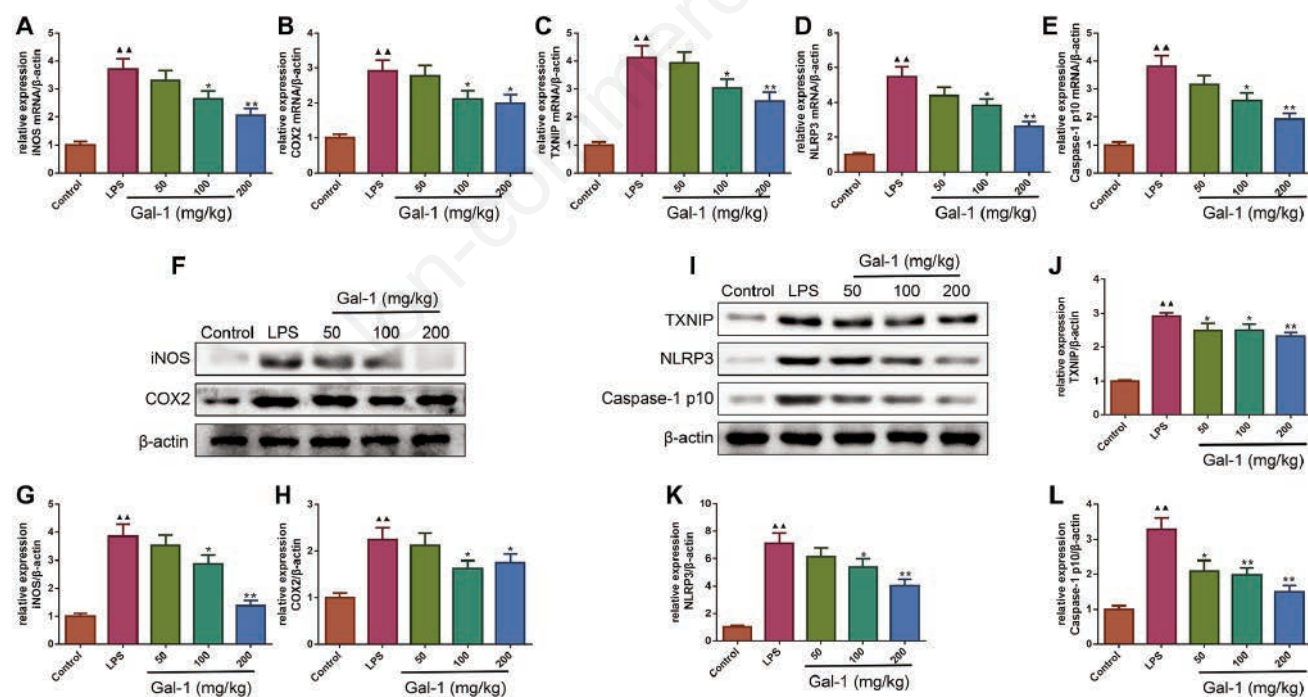


Figure 5. Pre-treatment with Gal-1 suppressed NLRP3 inflammasome activation in myocardial tissues induced by LPS. **A)** iNOS, **B)** COX2, **C)** TXNIP, **D)** NLRP3, and **E)** Caspase-1 p10 mRNA in the myocardial tissues were determined by qRT-PCR. **F)** Western blotting analysis of iNOS and COX2 protein expressions in myocardial tissues. **G-H)** Quantification of the iNOS and COX2 protein expressions in myocardial tissues. **I)** Western blotting analysis of TXNIP, NLRP3, and Caspase-1 p10 protein expressions in myocardial tissues. **J-L)** Quantification of the TXNIP, NLRP3, and Caspase-1 p10 protein expressions in myocardial tissues. ($\bar{x} \pm s$, $n=3$). ▲ $p < 0.05$, ▲▲ $p < 0.01$ vs Control group, ? $p < 0.05$, ?? $p < 0.01$ vs LPS group.

after LPS stimulation, but Gal-1 pre-treatment downregulated the trend. MDA is a suitable marker to reflect the damage degree of free radicals to the organism, and SOD is essential for the improvement of general redox and maintenance of intracellular homeostasis.²¹ As expected, the serum MDA concentration was obviously suppressed and the SOD activity was elevated by Gal-1 pre-treatment in myocarditis mice. Consistently, pre-treatment with Gal-1 decreased the fluorescence intensity of ROS *in vitro*. At the same time, in myocarditis, apoptosis is activated and related to the deterioration of cardiac function in patients with myocarditis,² and the myocardial cell apoptosis further induces cardiac injury and facilitates cardiac dysfunction.²² As shown by TUNEL staining and flow cytometry analysis *in vivo* and *in vitro*, Gal-1 pre-treatment exerted an antiapoptotic function on myocardial cells and displayed an outstanding cardioprotective function. These results suggested that Gal-1 might have an obvious protective effect on myocarditis by suppressing inflammation and oxidative stress.

Previous studies have revealed that NLRP3 inflammasome is vital in the development of myocarditis.²³ TXNIP is an essential multi-functional protein, which directly activates NLRP3 inflammasome, thereby further activating inflammation.²⁴ In the study, we found LPS stimulation obviously elevated TXNIP expression and activated NLRP3 inflammasome in the myocardium, while these situations were reserved by Gal-1 pre-treatment. These results indicated that Gal-1 pre-treatment prevents inflammation by repressing TXNIP-NLRP3 inflammasome activation. ROS is an important factor for activating NLRP3 inflammasome.²⁵ In a previous study, the NLRP3 inflammasome activation suppresses of Gal-1 was through reducing the ROS generation.²⁶ A similar result was obtained in this study.

Nrf2 plays a key role in cardioprotective combating oxidative stress.²⁷ And the cardioprotective properties of Nrf2 are predominantly correlated with Nrf2-dependent gene as well as protein expressions, such as HO-1.²⁸ HO-1 exhibits a potentially beneficial role in numerous cardiovascular diseases.²⁹ In the inactive state, Nrf2 stays in the cytoplasm by binding with Keap1. Some pharma-

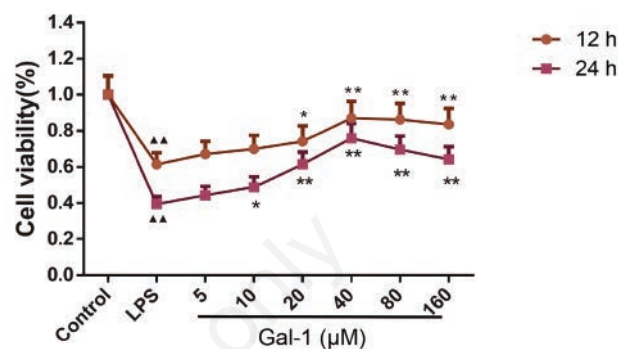


Figure 6. CCK-8 assay showed that Gal-1 pre-treatment prevented the reduction of cell viability in LPS-induced cells. ($\bar{x} \pm S$, $n=3$). \blacktriangle $p < 0.05$, $\blacktriangle\blacktriangle$ $p < 0.01$ vs Control group, * $p < 0.05$, ** $p < 0.01$ vs LPS group.

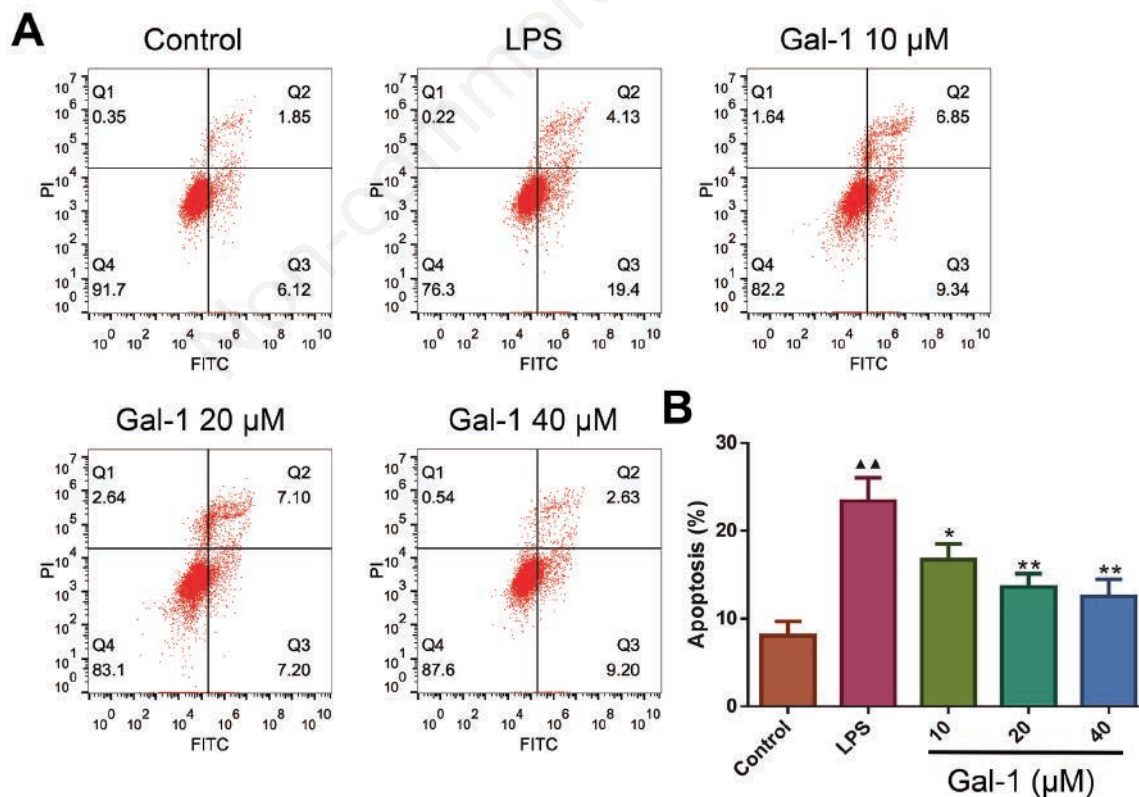


Figure 7. Effect of Gal-1 on LPS-induced apoptosis in H9c2 cells. **A)** Representative flow cytometry results obtained with annexin V-FITC. **B)** Data analysis showing apoptosis. ($\bar{x} \pm S$, $n=3$). \blacktriangle $p < 0.05$, $\blacktriangle\blacktriangle$ $p < 0.01$ vs control group, * $p < 0.05$, ** $p < 0.01$ vs LPS group.

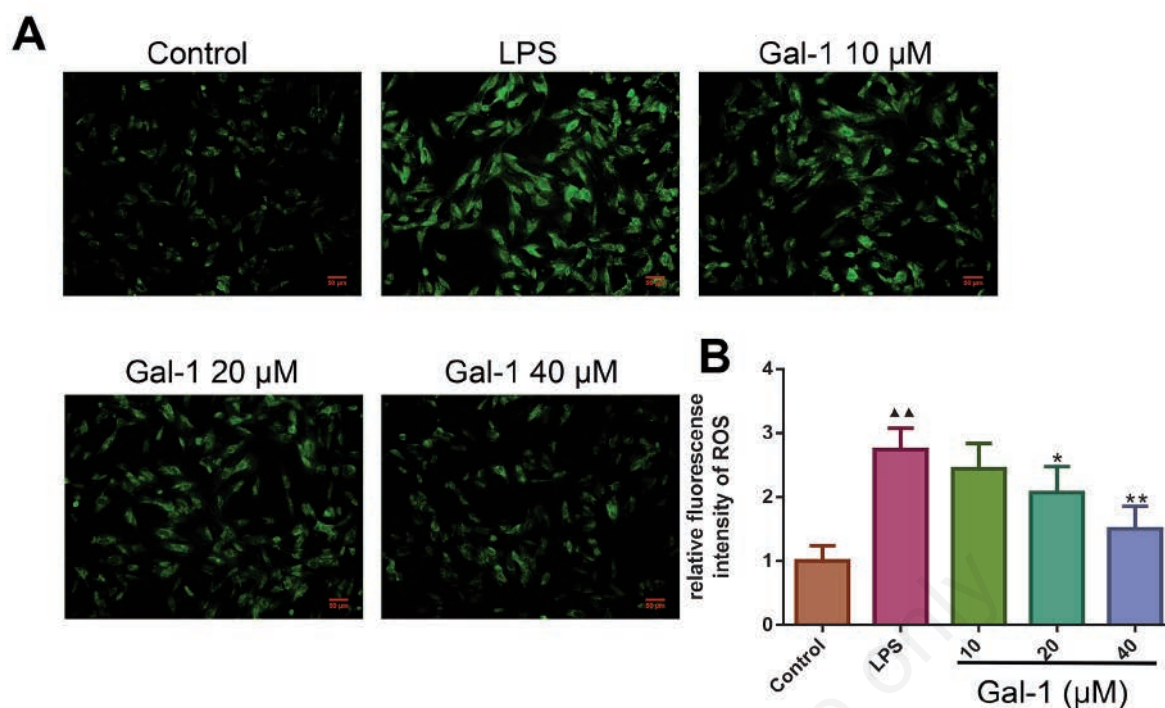


Figure 8. Gal-1 prevented H9c2 cells from oxidative stress injuries induced by LPS. **A)** Immunofluorescence assay showing the formation of intracellular ROS (stained by green fluorescence, original magnification $\times 100$). **B)** Quantitative analysis of the fluorescence intensity of ROS. ($\bar{x} \pm S$, $n=3$). $\blacktriangle p < 0.05$, $\blacktriangle\blacktriangle p < 0.01$ vs control group, $*p < 0.05$, $**p < 0.01$ vs LPS group.

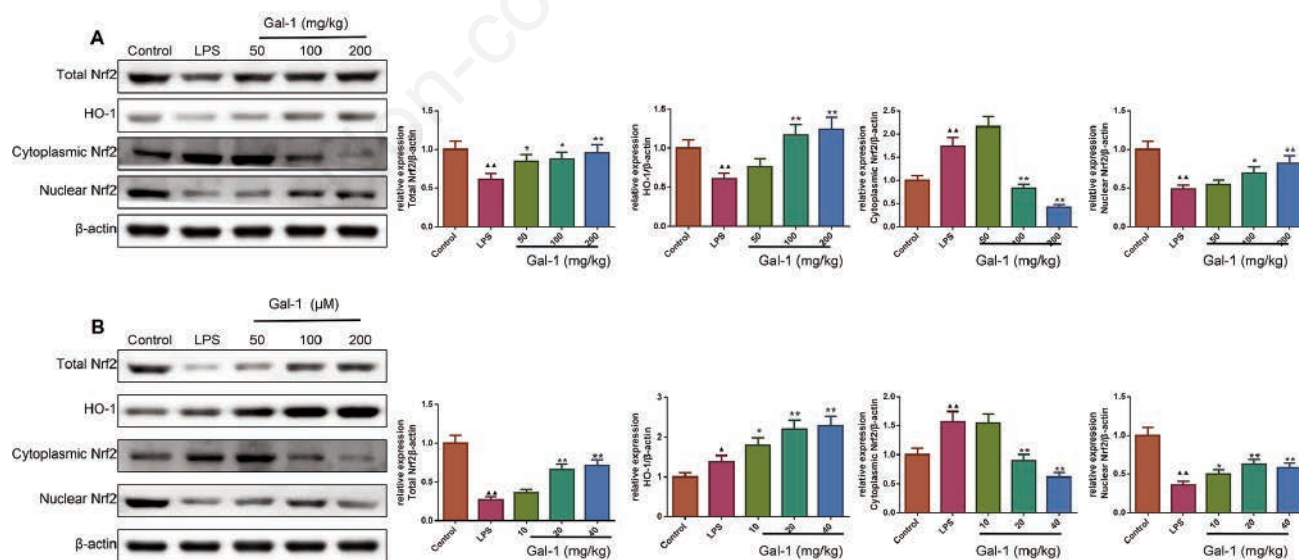


Figure 9. Effect of Gal-1 on Nrf2/HO-1 signaling in LPS induced myocardial tissue and H9c2 cells. **A)** Representative immunoblot and the expression of regulatory proteins, including total Nrf2, HO-1, cytoplasmic Nrf2 and nuclear Nrf2 in the myocardial tissues. **B)** Representative immunoblot and the expression of regulatory proteins, including total Nrf2, HO-1, cytoplasmic Nrf2 and nuclear Nrf2 in the H9c2 cells. ($\bar{x} \pm S$, $n=3$). $\blacktriangle p < 0.05$, $\blacktriangle\blacktriangle p < 0.01$ vs control group, $*p < 0.05$, $**p < 0.01$ vs LPS group.

cological as well as pathophysiological stimulation can deactivate Keap1, resulting in Nrf2 dissociating from Keap1 and translocating into nuclei.³⁰ Gal-1 pretreatment increased the total Nrf2 expression and nuclear translocation of Nrf2 in LPS-challenged myocardial tissues and H9c2 cells, indicating Nrf2 in cardiomyocytes was activated by Gal-1 pre-treatment. Meanwhile, Gal-1 pre-treatment also increased HO-1 protein expression in LPS-stimulated cardiomyocytes. These results implied that the Nrf2/HO-1 pathway might participate in the cardioprotective of Gal-1 in myocarditis.

The limitation of this study was that the experiment only examined the preventive effect of Gal-1 on LPS-induced myocarditis, and did not explore the potential role of Gal-1 in treating myocarditis. In the future, we will establish animal and cellular models of myocarditis with LPS again, and then treat myocarditis models with Gal-1, thereby further investigating the potential value of Gal-1 in myocarditis treatment.

In conclusion, our study suggested that Gal-1 pre-treatment had cardioprotective effects against myocarditis in model mice and H9c2 cells. And the cardioprotective effects of Gal-1 pre-treatment might contribute to the alleviation of inflammation as well as oxidative stress in myocardial tissues and inhibition of apoptosis in cardiomyocytes. In addition, Gal-1 exerted its cardioprotective effects on myocarditis by regulating the Nrf2 pathway and inhibiting the TXNIP-NLRP3 inflammasome. Therefore, this study provided potential choices for exploring novel drugs and targets for preventing acute myocarditis treatment.

References

- Chen L, Hou X, Zhang M, Zheng Y, Zheng X, Yang Q, et al. MicroRNA-223-3p modulates dendritic cell function and ameliorates experimental autoimmune myocarditis by targeting the NLRP3 inflammasome. *Mol Immunol* 2020;117:73-83.
- Fan S, Hu K, Zhang D, Liu F. Interference of circRNA HIPK3 alleviates cardiac dysfunction in lipopolysaccharide-induced mice models and apoptosis in H9C2 cardiomyocytes. *Ann Transl Med* 2020;8:1147.
- Hou X, Fu M, Cheng B, Kang Y, Xie D. Galanthamine improves myocardial ischemia-reperfusion-induced cardiac dysfunction, endoplasmic reticulum stress-related apoptosis, and myocardial fibrosis by suppressing AMPK/Nrf2 pathway in rats. *Ann Transl Med* 2019;7:634.
- Padappayil R, Chandini Arjun A, Vivar Acosta J, Ghali W, Mughal M. Acute myocarditis from the use of selective androgen receptor modulator (SARM) RAD-140 (testolone). *Cureus* 2022;14:e21663.
- Al-Obaidi N, Mohan S, Liang S, Zhao Z, Nayak B, Li B, et al. Galectin-1 is a new fibrosis protein in type 1 and type 2 diabetes. *FASEB J* 2019;33:373-87.
- Naqvi M, Memon M, Jamil T, Naqvi S, Aimulajiang K, Gadahi J, et al. Galectin domain containing protein from *Haemonchus contortus* modulates the immune functions of goat PBMCs and regulates CD4⁺ T-helper cells in vitro. *Biomolecules* 2020;10:116.
- Brinchmann M, Patel D, Iversen M. The role of galectins as modulators of metabolism and inflammation. *Mediators Inflamm* 2018;2018:9186940.
- Hisrich B, Young R, Sansone A, Bowens Z, Green L, Lessey B, et al. Role of human galectins in inflammation and cancers associated with endometriosis. *Biomolecules* 2020;10:230.
- van der Hoeven N, Hollander M, Yildirim C, Jansen M, Teunissen P, Horrevoets A, et al. The emerging role of galectins in cardiovascular disease. *Vascul Pharmacol* 2016;81:31-41.
- Seropian I, Cerliani J, Toldo S, Van Tassel B, Ilarregui J, González G, et al. Galectin-1 controls cardiac inflammation and ventricular remodeling during acute myocardial infarction. *Am J Pathol* 2013;182:29-40.
- Wang R, Li D, Ouyang J, Tian X, Zhao Y, Peng X, et al. Leonurine alleviates LPS-induced myocarditis through suppressing the NF- κ B signaling pathway. *Toxicology* 2019;422:1-13.
- Liu Y, Lou G, Li A, Zhang T, Qi J, Ye D, et al. AMSC-derived exosomes alleviate lipopolysaccharide/d-galactosamine-induced acute liver failure by miR-17-mediated reduction of TXNIP/NLRP3 inflammasome activation in macrophages. *EBioMedicine* 2018;36:140-50.
- Steinl D, Xu L, Ochoa-Espinosa A, Punjabi M, Kaufmann B. Non-invasive contrast enhanced ultrasound molecular imaging of inflammation in autoimmune myocarditis for prediction of left ventricular fibrosis and remodeling. *PLoS One* 2019;14:e0224377.
- Jiang X, Tang Q, Zhang J, Wang H, Bai L, Meng P, et al. Autophagy-dependent release of zinc ions is critical for acute lung injury triggered by zinc oxide nanoparticles. *Nanotoxicology* 2018;12:1068-91.
- Paknahad M, Yancheshmeh F, Soleimani A. Cardiovascular complications of COVID-19 vaccines: A review of case-report and case-series studies. *Heart Lung* 2023;59:173-80.
- Dobrică E, Cozma M, Găman M, Voiculescu V, Găman A. The involvement of oxidative stress in psoriasis: a systematic review. *Antioxidants (Basel)* 2022;11:282.
- Hu Y, Wang J, Du W, Wu N, Wang S, Zhang C, et al. Antiresistin neutralizing antibody alleviates doxorubicin-induced cardiac injury in mice. *Dis Markers* 2022;2022:3040521.
- Chou M, Lee Y, Wang Y, Cheng S, Cheng H. Cytotoxic and anti-inflammatory triterpenoids in the vines and leaves of *Momordica charantia*. *Int J Mol Sci* 2022;23:1071.
- Zhao Q, Yin L, Zhang L, Jiang D, Liu L, Ji H. Chitoheptaose promotes heart rehabilitation in a rat myocarditis model by improving antioxidant, anti-inflammatory, and antiapoptotic properties. *Oxid Med Cell Longev* 2020;2020:2394704.
- Osonoi S, Mizukami H, Itabashi C, Wada K, Kudoh K, Igawa A, et al. Increased oxidative stress underlies abnormal pain threshold in a normoglycemic Japanese population. *Int J Mol Sci* 2020;21:8306.
- Wang L, Zhu L, Gong L, Zhang X, Wang Y, Liao J, et al. Effects of Activated charcoal-herb extractum complex on antioxidant status, lipid metabolites and safety of excess supplementation in weaned piglets. *Animals (Basel)* 2019;9:1151.
- Cao H, Yang B, Zhao Y, Deng X, Shen X. The pro-apoptosis and pro-inflammation role of LncRNA HIF1A-AS1 in Cocksackievirus B3-induced myocarditis via targeting miR-138. *Cardiovasc Diagn Ther* 2020;10:1245-55.
- Khodir A, Samra Y, Said E. A novel role of nifuroxazide in attenuation of sepsis-associated acute lung and myocardial injuries; role of TLR4/NLPR3/IL-1 β signaling interruption. *Life Sci* 2020;256:117907.
- Wang C, Xu Y, Wang X, Guo C, Wang T, Wang Z. Dl-3-n-butylphthalide inhibits NLRP3 inflammasome and mitigates Alzheimer's-like pathology via Nrf2-TXNIP-TrX axis. *Antioxid Redox Signal* 2019;30:1411-31.
- Wang B, Lim J, Kajikawa T, Li X, Vallance B, Moutsopoulos N, et al. Macrophage β 2-integrins regulate IL-22 by ILC3s and protect from lethal *Citrobacter rodentium*-induced colitis. *Cell Rep* 2019;26:1614-26.e5.
- Huang X, Liu W, Zhou Y, Sun M, Yang H, Zhang C, et al.

- Galectin-1 ameliorates lipopolysaccharide-induced acute lung injury via AMPK-Nrf2 pathway in mice. *Free Radic Biol Med* 2020;146:222-33.
27. Wang X, Wang Z, Wu H, Jia W, Teng L, Song J, et al. Sarcodon imbricatus polysaccharides protect against cyclophosphamide-induced immunosuppression via regulating Nrf2-mediated oxidative stress. *Int J Biol Macromol* 2018;120:736-44.
28. Yang M, Mao G, Ouyang L, Shi C, Hu P, Huang S. Crocetin alleviates myocardial ischemia/reperfusion injury by regulating inflammation and the unfolded protein response. *Mol Med Rep* 2020;21:641-8.
29. Huang K, Lin M, Hsu H, Hsu Y, Huang T, Lu I, et al. Pinocembrin reduces keratinocyte activation and ameliorates imiquimod-induced psoriasis-like dermatitis in BALB/c mice through the heme oxygenase-1/signal transducer and activator of Transcription 3 pathway. *Evid Based Complement Alternat Med* 2022;2022:7729836.
30. Yang J, Sun M, Yuan Q, Tang S, Dong M, Zhang R, et al. Keap1-Nrf2 signaling activation by Bardoxolone-methyl ameliorates high glucose-induced oxidative injury in human umbilical vein endothelial cells. *Aging (Albany NY)* 2020;12:10370-80.

Non-commercial use only

Received: 28 June 2023. Accepted: 20 November 2023.

This work is licensed under a Creative Commons Attribution-NonCommercial 4.0 International License (CC BY-NC 4.0).

©Copyright: the Author(s), 2023

Licensee PAGEPress, Italy

European Journal of Histochemistry 2023; 67:3816

doi:10.4081/ejh.2023.3816

Publisher's note: all claims expressed in this article are solely those of the authors and do not necessarily represent those of their affiliated organizations, or those of the publisher, the editors and the reviewers. Any product that may be evaluated in this article or claim that may be made by its manufacturer is not guaranteed or endorsed by the publisher.